

# Scanning Tunneling Microscope Induced Crystallization of Fullerene-like MoS<sub>2</sub>

M. Homyonfer,<sup>†</sup> Y. Mastai,<sup>†</sup> M. Hershinkel,<sup>‡</sup> V. Volterra,<sup>‡</sup> J. L. Hutchison,<sup>§</sup> and R. Tenne<sup>\*,†</sup>

Contribution from the Department of Materials and Interfaces, Weizmann Institute, Rehovot 76100, Israel, Department of Physics, Ben-Gurion University, P.O. Box 653, Beer-Sheva 84105, Israel, and Department of Materials, University of Oxford, Parks Road, Oxford OX1 3PH, U.K.

Received May 8, 1996<sup>⊗</sup>

**Abstract:** Amorphous precursors, like MoS<sub>3</sub> (WS<sub>3</sub>), were shown before to be an ideal precursor for the growth of inorganic fullerene-like material in a rather slow crystallization process which lasts anything from 1 h at 800–900 °C<sup>1,2</sup> to a few years at ambient conditions.<sup>3,4</sup> Using a few microsecond short electrical pulses from the tip of a scanning tunneling microscope, crystallization of amorphous MoS<sub>3</sub> (a-MoS<sub>3</sub>) nanoparticles, which were electrodeposited on a Au substrate into MoS<sub>2</sub> nanocrystallites with a fullerene-like structure (IF-MoS<sub>2</sub>), is demonstrated. The (outer) shell of each nanocrystallite is complete, which suggests that the reaction extinguishes itself upon completion of the crystallization of the MoS<sub>2</sub> layers. A completely different mode of crystallization is observed in the case of continuous a-MoS<sub>3</sub> films. Here tiny (2–3 nm thick) 2H-MoS<sub>2</sub> platelets are observed after the electrical pulse, suggesting a very rapid dissipation of the thermal energy through the gold substrate, in the continuous domain. Since the reaction mechanism in both cases is believed to be the same, it is likely that the main stimulus for the chemical reaction/crystallization of the IF material results from the slow heat dissipation from the nanoparticle. The exothermicity of the chemical reaction may further promote the rate of the process.

## Introduction

Nanoparticles of layered compounds are inherently unstable in the planar form and adopt polyhedral (fullerene-like) topologies upon crystallization. Conversion of metal oxide nanoparticles into fullerene-like MX<sub>2</sub> (M = W, Mo; X = S, Se) polyhedra and nanotubes has been demonstrated.<sup>1–6</sup> Spontaneous crystallization of hollow cage WS<sub>2</sub> polyhedra from amorphous WS<sub>3</sub> soot at room temperature was also observed within a few years time.<sup>3,4</sup> Irradiation of the sample with intense electron<sup>3,7</sup> and ion beams<sup>8</sup> accelerates the crystallization of fullerene and fullerene-like nanoparticles to a time scale measured in minutes. However, this is a rather aggressive process which must be carried out in a controlled atmosphere. The present report deals with the crystallization of fullerene-like MoS<sub>2</sub> nanocrystallites (IF-MoS<sub>2</sub>) from an amorphous MoS<sub>3</sub> (a-MoS<sub>3</sub>) precursor of nano-size dimensions at ambient conditions. A rather short electric pulse from a scanning tunneling microscope (STM) tip led to an abstraction of sulfur atoms and subsequent crystallization of fullerene-like nanoparticles. This

process is attributed to the local heating of the nanoparticle, which is amplified by the small size of the contact area between the precursor nanoparticles and the gold substrate, and also to the exothermicity of the chemical reaction.

## Experimental Section

For sample preparation, a 35 nm thick polycrystalline gold film was evaporated onto a quartz substrate at room temperature and then annealed for 12 h at 250 °C.<sup>9</sup> The textured film consisted of (111) oriented gold grains, ca. 0.25 μm in size. Subsequently, a discontinuous film consisting of a-MoS<sub>3</sub> nanoparticles was deposited on the gold substrate using a modification of a previous procedure.<sup>10</sup> The film was not uniform: in certain areas a-MoS<sub>3</sub> nanoparticles mostly having an oval shape were obtained, while in other areas a continuous film, consisting of Mo and S but with varying stoichiometry, was deposited. The film was prepared by electrochemical deposition from a bath of 0.1 M ammonium thiomolybdate and 0.05 M Na<sub>2</sub>SO<sub>4</sub> dissolved in an aqueous solution at pH 5 and a bias of 0.23 V vs saturated calomel electrode (SCE).<sup>10</sup> The size of the nanocrystallites depended strongly on the bath temperature, with the typical size varying between 130, 40, and 5 nm at 10, 0, and –10 °C, respectively. The films which were used in the present work were prepared at 0 °C. Ambient scanning tunneling microscope (STM) provided with a Pt/Ir tip was used in the experiments. The surface of the sample was carefully scratched at certain points which served as markers for the identification of the STM-treated zones during the subsequent TEM analysis.

STM imaging of the a-MoS<sub>3</sub>/Au surface was done with a tunneling current of about 0.5 nA and a positive tip bias of 1.5–2.7 V, compared with 0.2 V used for a pure gold film. Before applying the electric pulses, an area of ca. 50 × 50 nm<sup>2</sup> was defined on the sample. Pulses ranging between 4 and 9 V (tip positive) were applied to induce crystallization of the amorphous nanoparticles, while the tip was positioned a few angstroms above the sample. The duration of the pulses varied from 10 to 1000 μs. The system automatically stopped

<sup>†</sup> Weizmann Institute.

<sup>‡</sup> Ben-Gurion University.

<sup>§</sup> University of Oxford.

<sup>⊗</sup> Abstract published in *Advance ACS Abstracts*, August 1, 1996.

(1) Tenne, R.; Margulis, L.; Genut, M.; Hodes, G. *Nature* **1992**, *360*, 444.

(2) Margulis, L.; Salitra, G.; Tenne, R.; Talianker, M. *Nature* **1993**, *365*, 113.

(3) Hershinkel, M.; Gheber, L. A.; Volterra, V.; Hutchison, J. L.; Margulis, L.; Tenne, R. *J. Am. Chem. Soc.* **1994**, *116*, 1914.

(4) Margulis, L.; Tenne, R.; Iijima, S. *Microscopy, Microanalysis and Microstructures*; in press.

(5) Feldman, Y.; Wasserman, E.; Srolovitz, D. J.; Tenne, R. *Science* **1995**, *267*, 222.

(6) Feldman, Y.; Frey, G. L.; Homyonfer, M.; Lyakhovitskaya, V.; Margulis, L.; Cohen, H.; Hodes, G.; Hutchison, J. L.; Tenne, R. *J. Am. Chem. Soc.* In press.

(7) Ugarte, D. *Nature* **1992**, *359*, 707.

(8) Chadderton, L. T.; Fink, D.; Gamaly, Y.; Moeckel, H.; Wang, L.; Omichi, H.; Hosoi, F. *Nucl. Instrum. Methods Phys. Res.* **1994**, *B91*, 71.

(9) Golan, Y.; Margulis, L.; Rubinstein, I. *Surf. Sci.* **1992**, *264*, 312.

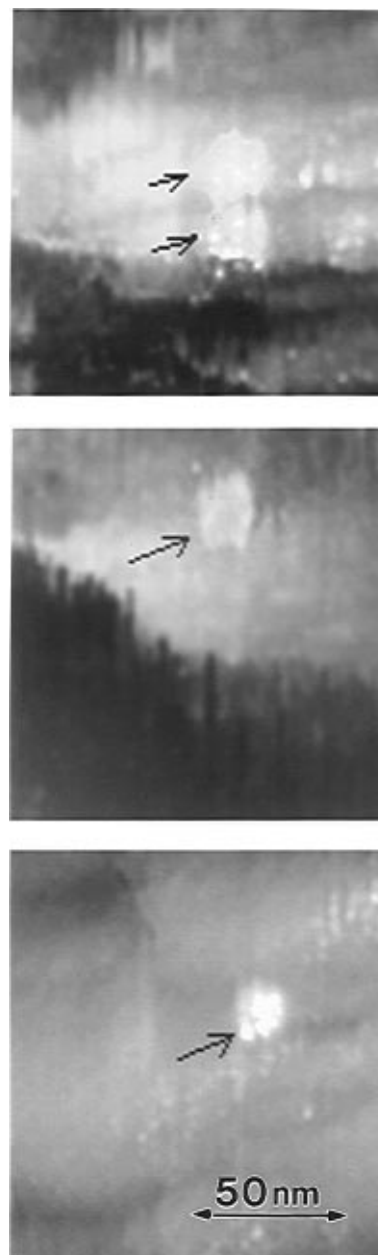
(10) Bélanger, D.; Laperrière, G.; Marsan, B. *J. Electroanal. Chem.* **1993**, *347*, 165.

the scanning prior to the pulse. During the pulse, the feedback loop was disengaged and a sample-hold loop fixed the tip in its position. After the pulse was applied, the feedback system was reactivated and the scanning was resumed. The predefined area was scanned repetitively to verify that apart from the oblate objects which appeared as a result of the pulse, no other modifications on the sample surface had occurred. Usually a few series of scan/pulse/scan routines were applied for the same predefined area. Subsequently, another 50 × 50 nm<sup>2</sup> area was defined on the same sample and the same procedure was repeated, and so forth. In several cases, well-defined nanoscopic features appeared following the pulses while in other cases no change in the STM image was noticed after a series of pulses. This irregularity is not surprising in view of the heterogeneity of the sample surface as pointed out above. Quite often, a pulse caused an instability in the successive scans. This instability was attributed to a cluster of sulfur atoms, which detached from the a-MoS<sub>3</sub> particle (film) during crystallization and stuck to the tip (*vide infra*).

A Philips model EM400 transmission electron microscope (TEM) with beam voltage of 100 keV was used for the analysis of most of the samples, while a high-resolution transmission electron microscope (HRTEM) JEOL model 2010 (beam voltage 200 keV) equipped with an energy dispersive analyzer (EDS) Link model ISIS was used for imaging and compositional analysis of a few samples (±1% accuracy) only. The size of the EDS probe was varied between 3 and 5 nm and the takeoff angle of the detector was changed. The results of the quantitative analysis were not influenced by varying the size of the probed zone or the takeoff angle. In order to peel-off the sample from the substrate without damaging it or the markers and transfer it onto the TEM grids, the sample edges were dipped briefly into a dilute (ca. 10%) HF solution. As soon as the edges of the thin gold film detached from the quartz, it was lifted-off completely very carefully and put on a grid with alpha-numerical markers, so that the STM treated zone could be easily identified under the TEM (HRTEM). This procedure permitted exact identification of the STM-treated zone without any difficulty. Prior to that, an alternative procedure was used according to which the identification of the treated zone was tedious and required prolonged examination of the sample with TEM/HRTEM, and was furthermore not always successful. The atomic percent content of each nanoparticle, which was based on the data collected by the EDS analyzer, was determined using the quantitative Cliff–Lorimer method for thin sections.

## Results

Since a-MoS<sub>3</sub> is insulating, STM imaging of the nanoparticles or the continuous film was not possible. For this reason, TEM and later on HRTEM were the most useful means for direct imaging of the nanoparticles and the film. Following the electrical pulse, typically 20 nm round objects were identified by the STM (Figure 1). The contour of the STM tip across such a nanoparticle was quite spherical indeed. Atomically resolved images of these objects could not be obtained with the STM, due likely to the curvature of the objects which implies that tunneling from more than one atom of the STM tip to the sample (and *vice versa*) takes place. The STM images resemble the ones reported before,<sup>3</sup> but it was not possible to decide whether the synthesis yielded nanoparticles with fullerene-like structure, at this stage. However, the appearance of such objects after the electrical pulses served as a criterion for the success of such experiments and only such samples were further analyzed by TEM, etc. To get a better idea of the structure of the nanoparticles, the treated sample was carefully transferred onto a polymer coated Cu grid and a TEM analysis was carried out. Figure 2a shows a TEM image of a group of amorphous oval a-MoS<sub>3</sub> nanoparticles deposited on the textured gold film. The average size of the nanoparticles is approximately 30 nm. Smaller a-MoS<sub>3</sub> nanoparticles are often observed (see inset of Figure 2a). A TEM image of a typical group of fullerene-like IF-MoS<sub>2</sub> particles, which were obtained after a series of electrical pulses were applied to the original film, is shown in



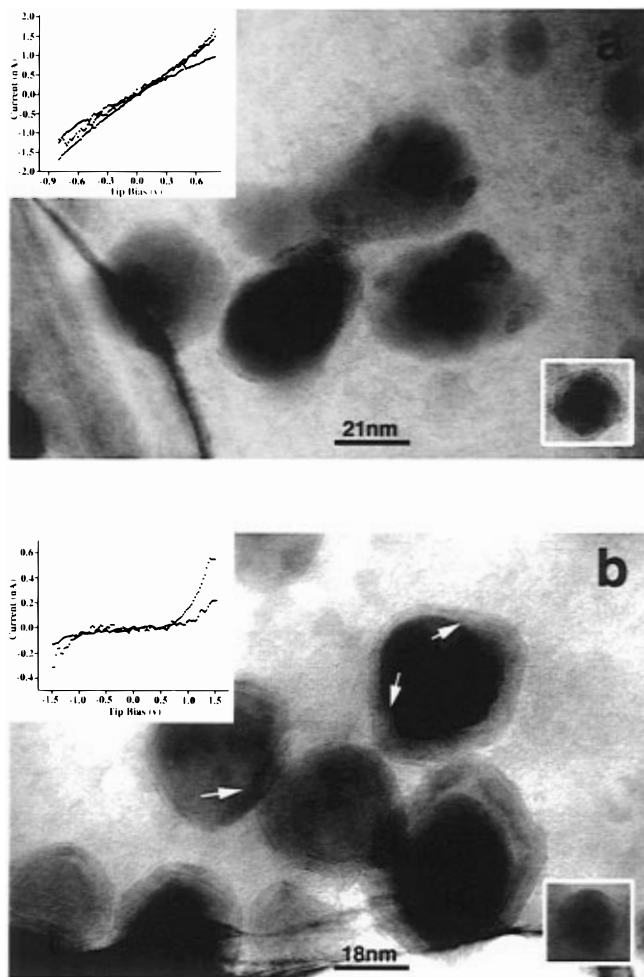
**Figure 1.** STM images of assortments of IF-MoS<sub>2</sub> nanoparticles produced by electrical pulse from the tip of the STM. Pulse voltage was 5 V in these experiments. The nature of each of the IF particles was verified through the semiconductor behavior of the I–V curve.

Figure 2b. Note that in most cases, the core of the nanoparticles remained amorphous. In the inset of Figure 2b a 15-nm nanoparticle is shown, which has been fully converted from a-MoS<sub>3</sub> into IF-MoS<sub>2</sub>. Growth fronts of the crystalline phase inside the amorphous core can be discerned (marked by arrows). Pulse experiments on top of the continuous nonstoichiometric Mo–S film or with pulse voltage smaller than 4 V did not lead to crystallization of fullerene-like structures (see also refs 11 and 12). Contrarily, pulses of 5 V and above produced fullerene-like objects, reproducibly. Complete destruction of the film surface and usually loss of an image was obtained with a pulse voltage larger than 8 V. The topology of the nested fullerene-like objects resembled structures reported earlier.<sup>1–6</sup>

Contrary to this behavior, a completely different mode of crystallization was observed for areas which were covered by

(11) Schimmel, Th.; Fuchs, H.; Lux-Steiner, M. *Phys. Status Solidi A* **1992**, *131*, 47.

(12) Akari, S.; Möller, S.; Dransfeld, K. *Appl. Phys. Lett.* **1991**, *59*, 243.



**Figure 2.** (a) TEM image of a group of  $\alpha$ - $\text{MoS}_3$  nanoparticles. In the insets are shown an amorphous particle of ca. 15 nm and a typical I–V curve obtained with this film. (b) Crystalline IF- $\text{MoS}_2$  nanoparticles with an  $\alpha$ - $\text{MoS}_3$  core. The insets show a fullerene-like nanoparticle of ca. 15 nm and a typical I–V curve obtained while the tip was fixed a few angstroms above one of the nanoparticles.

a continuous thin film of  $\alpha$ - $\text{MoS}_3$ . As shown in Figure 3, small 2H- $\text{MoS}_2$  platelets, which were embedded in the amorphous matrix, were formed as a result of the electrical pulse. The size of the crystalline domain is rather small (2–3 nm thick) in this case. The dissipation of the thermal energy, deposited by the electrical pulse in the continuous Mo–S film, was probably very fast and hence the energy density was below the required threshold for sulfur abstraction and crystallization of the material. Attempts to use the same method to obtain IF structures from large area  $\text{MoS}_2$  crystals were not successful. This result clearly indicates that IF- $\text{MoS}_2$  could occur only in discontinuous nanoscopic  $\alpha$ - $\text{MoS}_3$  domains of a diameter smaller than ca. 50 nm.

Prior to the application of the electrical pulses, an Ohmic behavior was observed for the film (inset of Figure 2a). The I–V curve, which was measured while the tip was fixed above fullerene-like nanoparticles (inset of Figure 2b), exhibited a typical semiconductor-like behavior with a statistically averaged bandgap of  $-1.1$  eV ( $\pm 0.05$  eV).<sup>3</sup> The value of the bandgap is ca. 0.1 eV smaller than the bandgap of the bulk (2H) material and was confirmed by direct optical measurements.<sup>13</sup> The shape of the I–V curve, which changed from a metallic-like behavior to a semiconductor-like behavior, was another criteria used to

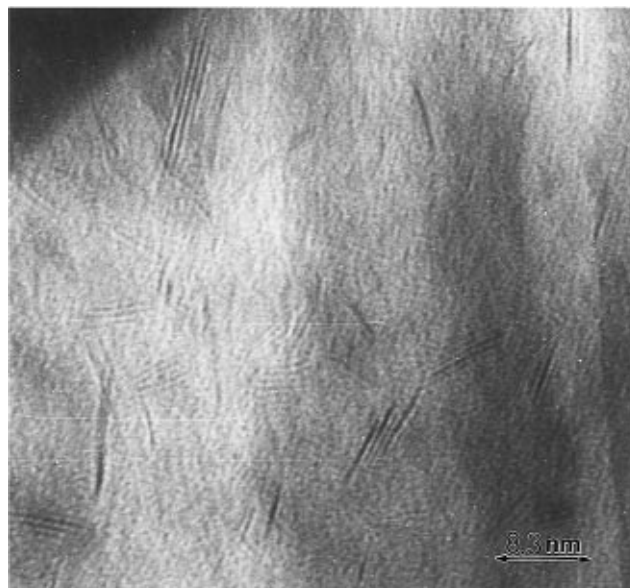


**Figure 3.** TEM image of a continuous nonstoichiometric Mo–S film on which a series of a few electrical pulses were applied and led to the crystallization of 2H- $\text{MoS}_2$  nano-size (ca. 2–3 nm) platelets.

judge the success of an experiment. The van der Waals surface of  $\text{MoS}_2$  is known to be very inert against oxidation, which is probably the reason for the fact that atomic resolution for the 2H polytype and meaningful values for the bandgap can be reproducibly obtained with ambient STM.<sup>3</sup>

Unfortunately, it is not possible to determine the accurate tip position with respect to the nanoparticle, while the electrical pulse was applied. Furthermore, the size of the IF particles did not seem to depend on the pulse potential (between 5 and 8 V), which indicates that their size is determined by the size of the precursor ( $\alpha$ - $\text{MoS}_3$ ) nanoparticles. This observation is not unique to the present process, since the size of the IF particles, which were produced from an oxide precursor, was also found to depend solely on the size of the precursor nanoparticles.<sup>6</sup> This analogy is not surprising in view of the fact that in both cases the crystallization goes from the outside to the inside.

In order to get more information about the process, HRTEM/EDS were used to analyze the samples prior to and after the electrical pulses. The high resolution of the microscope, coupled with the small thickness of the film and substrate, permitted chemical analysis of the nanoparticles one by one. Figure 4a shows a typical EDS spectrum taken from a single  $\alpha$ - $\text{MoS}_3$  nanoparticle, while Figure 4b shows a typical EDS spectrum of a single IF- $\text{MoS}_2$  particle. Apart from the contributions of the gold substrate, the Cu grid, and the constituting elements of the nanoparticles, no other foreign element could be detected. Table 1 shows the calculated atomic ratios of the various elements of the two typical nanoparticles. While the ratio of S/Mo was found to be 3.0 for the amorphous nanoparticles, the ratio varied between 1.8 and 2.2 for the nanoparticles with IF structure, in accordance with the hypothesized mechanism. Note that the contribution of the Cu grid stems from the large cross section of this metal with respect to X-ray emission.

Modifications of materials by pulse from the STM tip have been published.<sup>15–18</sup> The main mechanisms proposed for the process are field emission of electrons and atoms, deposition

(14) Srolovitz, D. J.; Safran, S. A.; Homyonfer, M.; Tenne, R. *Phys. Rev. Lett.* **1995**, *74*, 1799.

(15) Stauffer, U.; Wiesendanger, R.; Eng, L.; Rosenthaler, L.; Hidber, H. R.; Güntherodt, H.-J.; Garcia, N. *Appl. Phys. Lett.* **1987**, *51*, 244.

(13) Frey, G. L.; Homyonfer, M.; Feldman, Y.; Tenne, R. To be submitted for publication.

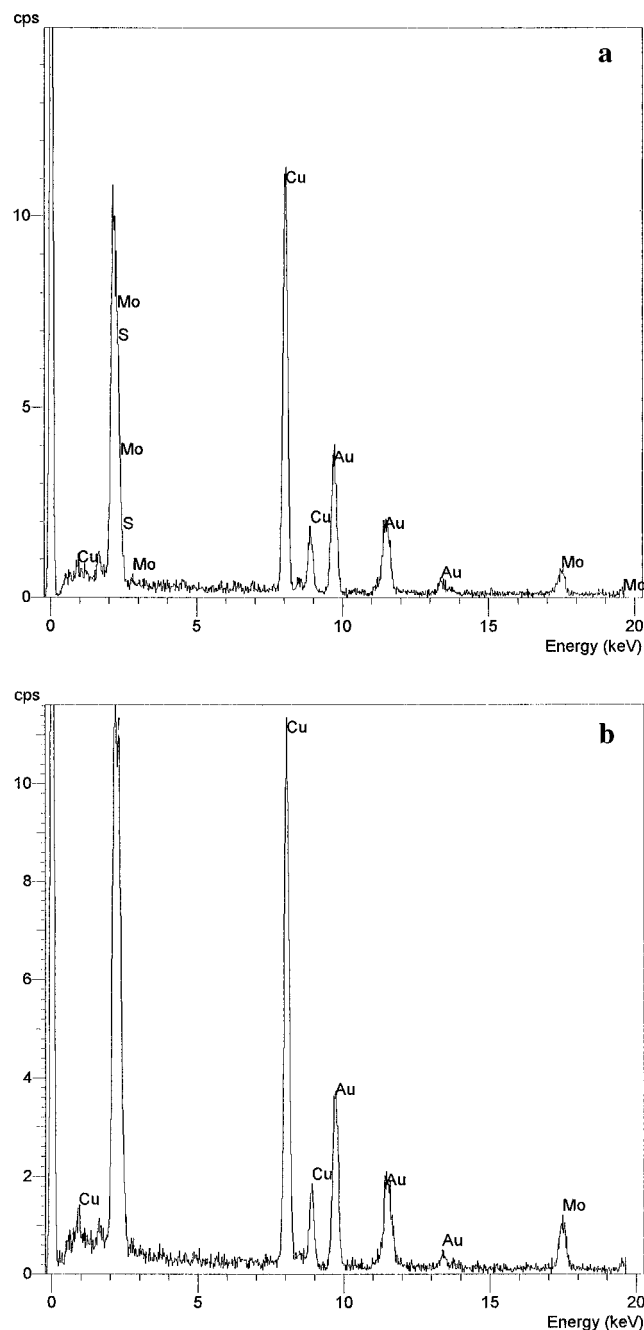


**Figure 4.** EDS spectra of a single nanoparticle: (a) IF-MoS<sub>2</sub>; (b) a-MoS<sub>3</sub>. Quantitative calculations of the nanoparticle composition were made using the data collected in these experiments.

of thermal energy,<sup>16</sup> and vibrational excitation of surface atoms.<sup>18</sup> Alternatively, the reaction can be initiated by pulse-induced cleavage of oxygen and water molecules and formation of O<sup>•</sup> and OH<sup>•</sup> radicals. In the absence of data for the heat conductivity and heat capacity of MoS<sub>3</sub>, the temperature rise cannot be calculated. Rough estimates for the temperature rise in amorphous metals under a similar pulse were as high as 1000 °C.<sup>16</sup>

In order to crystallize, each MoS<sub>3</sub> molecule in the nanoparticle must first lose one sulfur atom: MoS<sub>3</sub> → MoS<sub>2</sub> + S ( $\Delta G^\circ = -6.2$  kcal/mol<sup>19</sup>). This reaction is well documented in the

(16) Stauffer, U.; Wiesendanger, R.; Eng, L.; Rosenthaler, L.; Hidber, H. R.; Güntherodt, H.-J.; Garcia, N. *J. Vac. Sci. Technol. A* **1988**, *6*, 537.

(17) Parkinson, B. *J. Am. Chem. Soc.* **1990**, *112*, 7498.

(18) Shen, T. C.; Wang, C.; Abeln, G. C.; Tucker, J. R.; Lyding, J. W.; Avouris, P.; Walkup, R. E. *Science* **1995**, *268*, 1590.

**Table 1.** Compositional EDS Analysis of a Single Nanoparticle before and after the Application of an Electrical Pulse from the STM Tip

element	X-ray line	mol %	
		before the pulse	after the pulse
S	K	25.8	15.9
Cu	K	49.7	58.5
Mo	L	8.6	7.3
Au	M	15.9	18.3

literature.<sup>20</sup> Since the reaction is carried out in ambient conditions, an alternative pathway involving sulfur abstraction by oxygen is possible: MoS<sub>3</sub> + O<sub>2</sub> → MoS<sub>2</sub> + SO<sub>3</sub> (ΔG° = -77.6 kcal/mol<sup>19</sup>) and MoS<sub>3</sub> + <sup>3</sup>/<sub>2</sub>O<sub>2</sub> → MoS<sub>2</sub> + SO<sub>3</sub> (ΔG° = -94 kcal/mol<sup>19</sup>). Although all processes are exothermic, the oxygen-induced reactions are appreciably more favorable, and the evolution of gaseous SO<sub>2</sub> (SO<sub>3</sub>) drives the reaction to completion. However, the latter reactions might be kinetically hindered by a shortage of oxygen, particularly for the crystallization of the inner MoS<sub>2</sub> layers.

Previously, a slow conversion of tungsten (molybdenum) oxide into fullerene-like sulfide<sup>5,6</sup> was observed. The rate-determining step in this process was attributed to the intercalation of sulfur in the topmost sulfide layers and its slow diffusion toward the growth front inside the nanoparticle. The fast process observed in the present experiment suggests a different growth mechanism for the fullerene-like particles.

The outermost layers of the fullerene-like nanoparticles are found to be always complete. Also, the size and morphology of the fullerene-like nanoparticles do not seem to be influenced by the duration of the STM pulse. These facts indicate that the reaction starts at some point on the outer surface of the amorphous MoS<sub>3</sub> nanoparticle and is only terminated when the MoS<sub>2</sub> layers enveloping the surface are completed. These observations could possibly suggest a self-sustained, self-extinguishing mechanism which is reminiscent of the metathesis reactions between alkali sulfide and molybdenum (tungsten) halides.<sup>21</sup> Although the exothermicity of the metathesis reactions is appreciably larger, the present reaction produces heat in constricted domains of 15–40 nm. The heat cannot be effectively dissipated to the gold substrate, due to the small contact area between the spherical nanoparticle and the flat gold substrate film. Radiative emission to the ambient atmosphere is also rather slow. Therefore, the energy density, which is released during the electrical pulse, is likely to be even higher than the metathesis reaction and the reaction can therefore self-sustain itself. The local heating of the nanoparticle provides also the necessary energy to form the point defects, which are responsible for the bending of the otherwise flat surface of the hexagonal network.<sup>1,22</sup> Once the fullerene-like shell is completed the reaction is switched off automatically. The threshold bias of 4 V is required for the initial abstraction of sulfur atoms through one of the above mechanisms. These atoms may remain on the STM tip surface and induce current instability, which is often observed after the pulse.

On the other hand, the crystallization of the continuous film is interrupted very shortly after the pulse, and the domain size of the 2H-polytype nanocrystallites is very small (ca. 2–3 nm)

(19) *Standard Potentials in Aqueous Solution*; Bard, A. J., Parsons, R., Jordan, J., Eds.; Marcel Dekker: New York, 1985.

(20) Elliott, R. P. *Constitution of Binary Alloys, First Supplement*; McGraw-Hill: New York, 1965; p 632.

(21) Bonneau, P. R.; Jarvis, R. F., Jr.; Kaner, R. B. *Nature* **1991**, *349*, 510.

(22) Zhang, Q. L., et al. *J. Phys. Chem.* **1986**, *90*, 525. Kroto, H. W. *Nature* **1987**, *329*, 529.

in this case, which suggests that the local heating of this sample due to the electrical pulse is confined to a very small domain and excludes a self-sustained reaction here. Most of the heat is shunted through the gold film which serves as a substrate for the Mo–S film. The large contact area between these two films facilitates the heat transfer across the interface. The size of the 2H platelets can be influenced also by the irregular composition (S/Mo ratio) in the film. There is no reason to believe that the reaction mechanism for the sulfur abstraction in the continuous film is very different from the mechanism in the discontinuous nanocrystallites and hence the same mechanism for crystallization should pertain for both cases. This argument indicates that the slow dissipation of electrical (thermal) energy from the amorphous nanoparticle leads to a very strong local heating of the nanoparticle which is responsible for the thermally activated process:  $\text{MoS}_3 \rightarrow \text{IF-MoS}_2 + \text{S}$ .<sup>20</sup>

In conclusion, very short electrical pulses from an STM tip were applied to amorphous  $\text{MoS}_3$  nanoparticles and induced fast crystallization of an amorphous precursor into fullerene-like  $\text{MoS}_2$  particles in ambient conditions. A mechanism for this unique process has been proposed. A Schottky-like junction between the fullerene-like  $\text{MoS}_2$  nanoparticle and the supporting Au film has been established and is currently investigated.

**Acknowledgment.** We are grateful to Prof. M. Talianker and Mr. V. Ezersky of the Department of Materials Engineering, Ben-Gurion University, Beer-Sheva. We also thank Drs. S. Cohen and H. Cohen of the Department of Chemical Services of the Weizmann Institute for the suggestions regarding the paper. This research was supported by the Israeli Ministry of Science and the Arts, Ministry of Energy and Infrastructure and the UK–Israel Science and Technology Fund.

JA961544X